# Scalings and Relative Scalings in the Navier-Stokes Turbulence

Nianzheng Cao,[1,2] Shiyi Chen,[1,2] and Zhen-Su She[3,4]
[1]*IBM Research Division, T. J. Watson Research Center, P.O. Box 218, Yorktown Heights, New York 10598*
[2]*Theoretical Division and Center for Nonlinear Studies, Los Alamos National Laboratory, Los Alamos, New Mexico 87545*
[3]*Department of Mathematics, University of Arizona, Tuscon, Arizona 85721*
[4]*Department of Mathematics, University of California, Los Angeles, California 90095*
(Received 28 August 1995; revised manuscript received 6 March 1996)

High-resolution direct numerical simulations of 3D Navier-Stokes turbulence with normal viscosity and hyperviscosity are carried out. It is found that the inertial-range statistics, both the scalings and the probability density functions, are independent of the dissipation mechanism, while the near-dissipation-range fluctuations show significant structural differences. Nevertheless, the relative scalings expressing the dependence of the moments at different orders are universal, and show unambiguous departure from the Kolmogorov 1941 description, including the $2/3$ law for the kinetic energy. Implications for numerical modeling of turbulence are discussed. [S0031-9007(96)00251-7]

PACS numbers: 47.27.Gs

The Kolmogorov 1941 similarity theory (K41) [1] of fully developed turbulence assumes the existence of universal statistics of fluctuations at so-called inertial-range scales $\ell_0 \gg \ell \gg \ell_d$, where $\ell_0$ and $\ell_d$ are the characteristic length scale of the kinetic energy and dissipation, respectively. This hypothesis has a series of implications, including the prediction of the independence of the inertial range on the dissipation mechanism, and the $2/3$ law for the kinetic energy fluctuations $\langle \delta u_\ell^2 \rangle \sim \ell^{2/3}$. Physically, the inertial range is defined by the condition that the mean energy flux is constant. It is known that a constant energy flux range may exist with anomalous scaling behavior, the so-called intermittency effects [2–4]. However, accurate numerical determination of the inertial-range scaling exponents has been a great challenge due to the finite-range size effects and statistical convergence.

Recently, the question has been raised as to whether or not the observed large-scale statistical features depend on the mechanism of the energy dissipation [5,6]. Answering this question has significant impact on the numerical modeling of turbulence and the understanding of fundamental physics in fluid turbulence. For nearly all flows of practical and engineering interest, it is impossible in the foreseeable future to numerically resolve all scales from $\ell_0$ to $\ell_d$ using the Navier-Stokes equations. In one way or another, some artificial damping mechanism must be introduced at a length scale of the numerical resolution $\ell_g$. Whether and how such modeling affects the large-scale dynamics ($\ell > \ell_g$) is a key issue to the success of the numerical modeling. The existence of universality was often assumed in previous studies without documented evidence [4,7].

Leveque and She [5] have recently examined this issue using a model system of fully developed turbulence, the so-called GOY (Gledzer-Ohkitani-Yamata) shell model [8]. This model is a dynamical system with a chain interaction linking fluctuations at various scales. In the statistically stationary state, the system displays a cascade of energy to larger wave-number shells, which are characterized by anomalous scaling behavior [9] similar to what is observed in real turbulence [10]. It is shown [5] that the scaling of the inertial range in the GOY shell model (over 2 decades) depends on a hyperviscosity index $h$ (see below), whereas other features such as relative scaling (see below) remain universal. The hyperviscosity has also been applied to 3D Navier-Stokes turbulence by Borue and Orszag [4]. There is speculation that this dependence of the inertial range behavior on dissipation might also survive in the 3D Navier-Stokes turbulence [6]. If so, the traditional concept of universality of the inertial range would be challenged. Since most scaling theories are based on K41, it is extremely important to resolve this issue.

In the present study, we have carried out a detailed comparison of the statistics of isotropic turbulence generated by the Navier-Stokes equations with normal and hyperviscous damping. Particular emphasis was given to the scaling dynamics. The hyperviscous damping is expressed in the wave-number space by $\nu_h |k|^{2h}$. When $h = 1$, this is the normal damping for a Newtonian fluid. As $h \to \infty$ and $\nu_h = \nu_0 k_d^{-h} \to 0$, the hyperviscous term introduces infinite dissipation above the wave number $k_d$, and almost none below. In physical space, such hyperviscous damping corresponds to a coupling which diffuses excitations in an undulatory way. The specific questions to be addressed include to what extent does a hyperviscous field represent a high-Reynolds-number turbulent field? What are the properties that are independent of the viscous damping mechanisms in the 3D Navier-Stokes dynamics?

The main results are as follows: (1) The statistics at near-dissipation-range scales ($\ell \approx \ell_d$) are considerably modified by the presence of the hyperviscous damping, but at inertial-range scales there seem to be little affected in the 3D Navier-Stokes dynamics (this result is to be contrasted to the shell model case). (2) While the normal viscous damping is unable to provide a clear inertial range even with today's highest Reynolds number achievable ($\mathrm{Re}_\lambda \approx 210$), the hyperviscous damping ($h > 1$) does display an inertial range which exhibits clear departure from the K41 description. (3) There appears to be universal relative scaling independent of the damping mechanism, which deviates also unambiguously from the K41 description. (4) The energy spectra in the Fourier space $E(k)$ for normal viscous fields are affected through the whole range by so-called "bottleneck" effects, whereas the hyperviscous fields show a finite inertial range with exponents which cannot be directly related to the ones obtained from the second-order velocity structure functions in the physical space. Further investigations are needed to assess the impact on the measured scaling exponents (see [11]).

The 3D incompressible Navier-Stokes equations with a hyperviscous damping, written as

$$\partial \mathbf{u}/\partial t + \nabla \cdot (\mathbf{u}\mathbf{u}) = -\nabla p + (-1)^{h+1} \nu_h \nabla^{2h} \mathbf{u},$$

$$\nabla \cdot \mathbf{u} = 0,$$

are solved numerically for the periodic boundary conditions. Here $p$ is the pressure. A pseudospectral code has been developed using a second-order time-integration scheme [12]. Simulations are carried out with resolutions of $256^3$ and $512^3$ on the CM-5 at Los Alamos National Laboratory and the SP machines at IBM T. J. Watson Research Center. To obtain a statistically steady state, a forcing is applied to the first wave-number shell $0.5 < k < 1.5$ so that at each time step the total energy of that shell is constant. Time integration up to 60 large-eddy turnover times is performed to collect data for the analysis of the statistical steady state.

The statistics of turbulent fields in the physical space are commonly characterized by the velocity structure functions (VSF) $U_p(\ell) = \langle |\delta u_\ell|^p \rangle$, where $\delta u_\ell$ is the velocity increment across a distance $\ell$. The velocity structure functions are moments of $\delta u_\ell$ evaluated from the probability density functions (PDFs), $P(\delta u_\ell)$. A somewhat different measure of the behavior of $P(\delta u_\ell)$ is the so-called flatness factor, $F_4(\ell) = U_4(\ell)/U_2(\ell)^2$, which indicates how "flat" the tails of the PDFs are. The higher the flatness factor, the flatter the PDFs and more large amplitude events are observed. In Fig. 1, we compare $F_4(\ell)$ for a normal viscous damping ($h = 1$) with that for $h = 2$ and $h = 8$ at all length scales. It can be clearly seen that, at large scales $\ell > 0.2$, the three cases approximately agree. The same result has also been obtained from hyperflatness factors $F_6(\ell)$, indicating that the shape of the PDFs does not sensitively depend on $h$ at large scales. On the other hand, at $\ell < 0.2$, we observe a systematic decrease of the flatness factors as $h$ increases, implying that, with a hyperviscous damping, the small-scale field becomes less intermittent. Our interpretation of this reduction of intermittency with hyperviscosity is as follows: Because the hyperviscous damping is more oscillatory, small-scale structures, such as vortices, are broken down into smaller pieces. The fragmented field has a more gentle variation, and therefore appears less intermittent. Nevertheless, this fragmentation does not seem to affect the large-scale coarse-grained structures, as evidenced by the agreement of the flatness factors at $\ell > 0.2$.

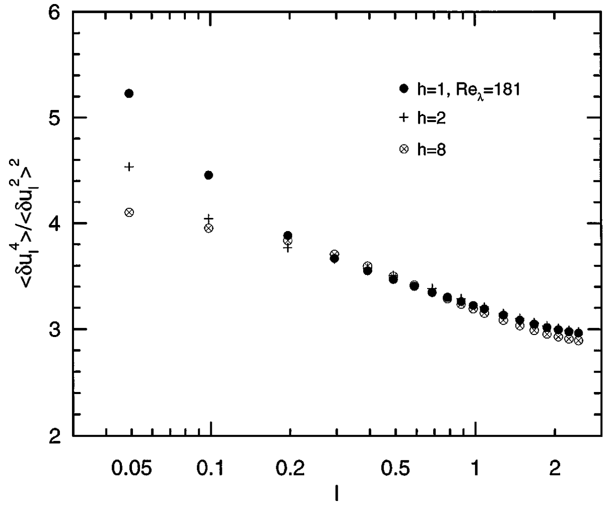


FIG. 1. Flatness of velocity increment as a function of separation, $\ell$, for $h = 1$, $h = 2$, and $h = 8$.

This observation may not be surprising, but it provides a solid ground for large-eddy numerical modeling of turbulent flows. It confirms that the effects of a hyperviscous damping on the form of PDFs do not propagate very far beyond the dissipation length scale in 3D incompressible fluids. The sharp difference from the GOY shell model may stem from the fact that the number of modes in each wave-number octave increases as $|k|^3$, so that many possible backward propagation events interfere with each other and cancel the effects. Similar ideas are suggested by Kraichnan [13].

A further characterization of the statistical state is the local rate of change of the velocity structure function, or the local scaling exponent $\zeta_p(\ell) = d \log \langle \delta u_\ell^p \rangle / d \log \ell$. Numerically, $\zeta_p(\ell)$ can be obtained by a least-squares fit over a small range of $\ell$'s, approximating the local slope in the log-log coordinate. In Fig. 2, we report $\zeta_2(\ell)$ and $\zeta_3(\ell)$ for the whole range of $\ell$ for $h = 2$. The data are obtained using a particularly large number of samples (~60 large-eddy turnover times). Here, we pay particular attention to the convergence issue, plotting $\zeta_p(\ell)$ with an increasing number of averaging frames. From this figure, we may easily identify a range where the local scaling exponent is constant. We believe that this is a legitimate definition of the inertial range. It is remarkable that $\zeta_2$ over this finite range converges to a value below $2/3$ with little uncertainty, as evidenced by the small difference between the values at 100, 150, and 200 frames. To our knowledge, this is the first solid numerical evidence supporting the intermittent scaling

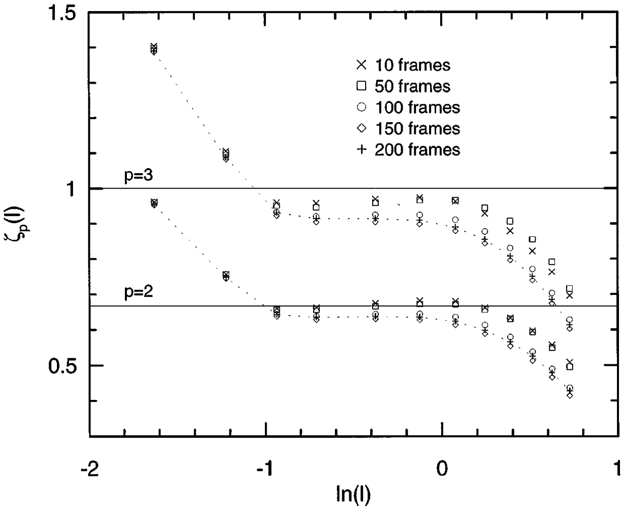


FIG. 2. Local scaling exponent, $\zeta_p(\ell) = d\ \log\langle\delta u_\ell^p\rangle/d\ \log\ell$ (for $p = 2$ and 3), as a function of separation $\ln(\ell)$ with an increasing number of samples for $h = 2$. The solid lines are from the K41 theory, and the dashed lines connect the final results obtained with 200 frames of $256^3$ field data collected over 60 large-eddy turnover times.

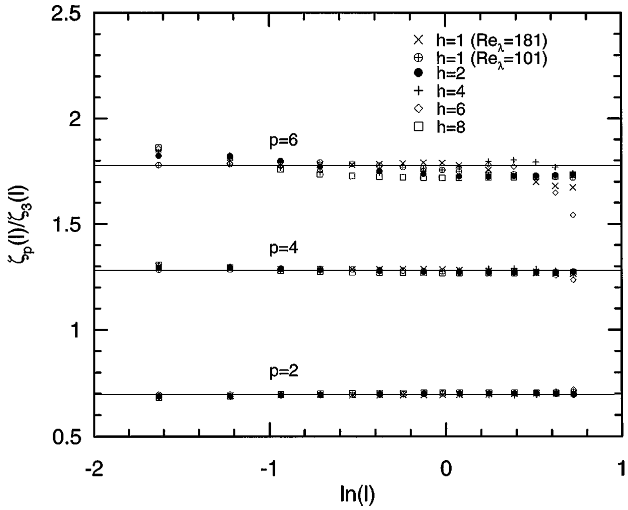


FIG. 3. Local relative scaling exponent $\zeta_p(\ell)/\zeta_3(\ell)$ at $p = 2, 4$, and 6, as a function of separation, $\ln(\ell)$, for different $h$'s. The solid lines are from Ref. [15].

correction for the second-order structure function. It is also clear that $\zeta_3$ converges to a value below unity. Note that what we examine here is the local scaling of the velocity structure function taking the *absolute* value of the velocity increments, so that the third-order moments do not necessarily scale linearly with the separation distance. Very similar results are obtained for $h = 8$ at the same range.

One may ask whether this range is asymptotic to infinite Reynolds number. We cannot provide a definite answer to this question numerically, nor any finite Reynolds number real-life experiments, but we must remark that this range, although finite, is physically very relevant because the energy flux is remarkably constant [4]. It may also be asked whether the scaling deviation from the 2/3 law is due to the use of hyperviscosity. We have examined this issue carefully. Due to the absence of an inertial range for the normal-viscous fields (even with the highest Reynolds number $\mathrm{Re}_\lambda \approx 210$), a firm conclusion for the scaling exponents cannot be reached directly. On the other hand, through the relative scaling exponents shown below, we do see strong evidence that the relative scaling exponents for second- and third-order structure functions depart from K41 in a similar way, regardless of the $h$ index, implying that the simulation results presented here are not the effect of hyperviscosity.

It is important to look for universal features which are independent of the dissipation mechanisms. In fact, the relative scaling exponent, such as $\zeta_p/\zeta_3 = d\ \log\langle\delta u_\ell^p\rangle/d\ \log\langle\delta u_\ell^3\rangle$, might be more fundamental than the scaling exponent itself in describing the properties of the cascade dynamics under nonlinear interaction, since it represents the relation between the fluctuations of different amplitudes through the variation of PDF as a function of spatial separation. Using relative scaling exponents in experimental measurement was first suggested by Benzi *et al.* [10], and it turns out to be a useful measure, and has stimulated many discussions [14]. Leveque and She [5] reported that, in the GOY shell model, the relative scalings are independent of the dissipation mechanism.

We have carried out measurements of the local relative scaling exponents and the results are shown in Fig. 3. It can be clearly seen that there exists an extended range over which the VSF behave as a power law; the local scaling exponents are constant. Here, we have collected data for several Reynolds numbers at normal viscosities, and for several hyperviscosities. The solid lines are the theoretical predictions of the She-Leveque model [15]. It is remarkable that the scaling exponents are universal and almost independent of the dissipation mechanisms. The values of these exponents for $\mathrm{Re}_\lambda = 181$ with normal viscosity are presented in Table I. They are in very good

TABLE I. Relative scaling exponent numerically calculated for $h = 1$, $\mathrm{Re}_\lambda = 181$, compared with theoretical results of K41 and She and Leveque (SL) [11].

| Order $p$ | $\zeta_p/\zeta_3$ (numerical) | K41 | SL model |
|---|---|---|---|
| 1 | 0.362 ± 0.003 | 0.333 | 0.364 |
| 2 | 0.695 ± 0.003 | 0.667 | 0.696 |
| 3 | 1.000 | 1.000 | 1.000 |
| 4 | 1.279 ± 0.004 | 1.333 | 1.280 |
| 5 | 1.536 ± 0.010 | 1.667 | 1.538 |
| 6 | 1.772 ± 0.015 | 2.000 | 1.778 |
| 7 | 1.989 ± 0.021 | 2.333 | 2.001 |
| 8 | 2.188 ± 0.027 | 2.667 | 2.211 |

agreement with the prediction of the She-Leveque model [15]. We emphasize that the deviation from the K41 prediction is quite clear, beyond numerical uncertainty, even for second order (the kinetic energy). In other words, the relative scaling exponents $\zeta_2/\zeta_3 \neq 2/3$.

Finally, we have examined the behavior of the energy spectrum in the Fourier space. In Fig. 4, we present compensated spectra for three cases with $h = 1$ ($\mathrm{Re}_\lambda =$ 101 and 181) and $h = 8$. We have chosen to plot $k^{5/3}E(k)$ [1] for $h = 1$ and $k^2E(k)$ for $h = 8$, to reveal a flat region at low wave number with $k < 20$. In order to judge the significance of the exponents, we plot, in the inset of Fig. 4, the local scaling exponent, $\alpha(k)$, defined by $E(k) \sim k^{\alpha(k)}$, or $\alpha(k) = d \log E(K)/d \log k$. It then becomes clear that no obvious constant $\alpha(k)$ range is present for $h = 1$; the exponent $-5/3$ stands for just a local averaged exponent over a finite range. For $h = 8$, there is a finite range near the dissipation falloff with an exponent $\alpha(k) \approx -1$. This range is commonly identified as the bottleneck range [16]. We believe that this range is formed by a reflection of the excitations from the dissipation cutoff. The difference between the GOY shell model and the 3D Navier-Stokes results is that this range extends to the whole inertial range in the former case. Indeed, it is observed that the bottleneck range becomes flatter as $h$ increases, similar to the GOY shell model [5]. For $h = 8$, a new scaling range seems to appear for $k < 10$, where the local exponent varies between $-1.8$ and $-2$ [4]. It is not clear, however, if the value is asymptotic. On the other hand, for the data with $h = 1$ and $\mathrm{Re}_\lambda \approx 181$, the whole large-scale spectrum ($3 < k < 20$) seems to be influenced by the bottleneck effect, as evidenced by the characteristic hump in $\alpha(k)$. This is consistent with the fact that no good power-law range is observed in $\langle \delta u_\ell^2 \rangle$ for $h = 1$ in the physical space. The trend of larger $\alpha$ can be also extracted from existing high Reynolds number experiments [17], consistent with our numerical observation. It is our belief that an even higher Reynolds number is required to obtain the "true" inertial range for normal viscosity.

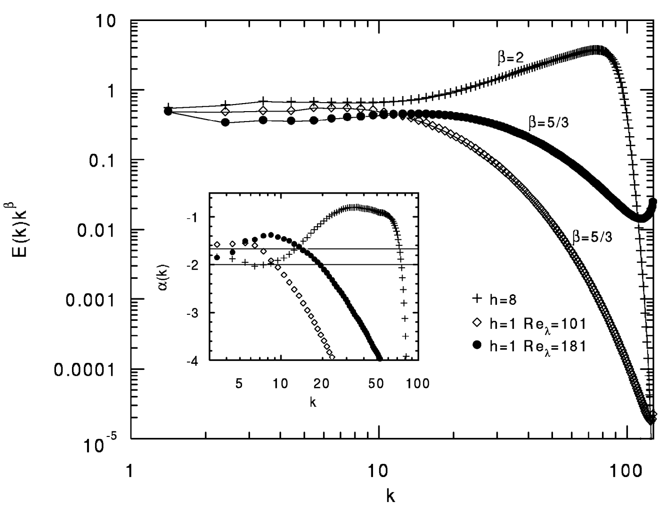


FIG. 4. Compensated energy spectra for $h = 1$ and $h = 8$. The inset shows the local scaling exponent of the energy spectra $\alpha(k)$ for the same runs. The solid lines in the inset are for $\alpha(k) = -5/3$ and $-2$, respectively.

We thank V. Borue, G. Doolen, R. Kraichnan, D. Lohse, D. Martinez, M. Nelkin, E. Pytte, and L. P. Wang for useful discussions. Part of this work was supported by the U.S. Department of Energy at Los Alamos National Laboratory. Numerical simulations were carried out at the Advanced Computing Laboratory at Los Alamos National Laboratory using the Connection Machine-5, and the Center for Scalable Computing Solution at IBM T. J. Watson Research Center using the SP machines. Z.-S. S. is partially supported by the Center for Fluid Dynamics at Princeton University, the IBM T. J. Watson Research Center, the Sloan Foundation, and the ONR under Contract 95431-0055.

[1] A. N. Kolmogorov, C. R. Acad. Sci. RUSS **30**, 301 (1941).
[2] A. Y. S. Kuo and S. Corrsin, J. Fluid Mech. **50**, 285 (1971); P. Kailasnath, K. R. Screenivasan, and G. Stolovitzky, Phys. Rev. Lett. **68**, 2766 (1992); A. Vincent and M. Meneguzzi, J. Fluid Mech. **225**, 1 (1991).
[3] Z.-S. She, S. Chen, G. Doolen, R. H. Kraichnan, and S. A. Orszag, Phys. Rev. Lett. **70**, 3251 (1993).
[4] V. Borue and S. A. Orszag, Europhys. Lett. **29**, 687 (1995).
[5] E. Leveque and Z.-S. She, Phys. Rev. Lett. **75**, 2690 (1995).
[6] L. P. Kadanoff, Phys. Today 11–13 (1995).
[7] J. Smagorinsky, Mon. Weather Rev. **91**, 99 (1963).
[8] E. B. Gledzer, Soc. Phys. Dokl. **18**, 216 (1973); M. Yamada and K. Ohkitani, J. Phys. Soc. Jpn. **56**, 4210 (1987); Phys. Rev. Lett. **60**, 983 (1988).
[9] E. Leveque and Z.-S. She (to be published).
[10] R. Benzi, S. Ciliberto, R. Tripiccione, C. Baudet, E. Massaioli, and S. Succi, Phys. Rev. E **48**, 29 (1993); M. Briscolini, P. Santangelo, S. Succi, and R. Benzi, Phys. Rev. E **50**, R1745 (1994); R. Benzi, S. Ciliberto, C. Baudet, G. Ruiz Chavaria, and R. Tripiccione, Europhys. Lett. **24**, 275 (1993).
[11] L. Kadanoff, D. Lohse, and J. Wang, Phys. Fluids **7**, 617 (1995).
[12] S. Chen, G. D. Doolen, R. H. Kraichnan, and Z.-S. She, Phys. Fluids A **5**, 458 (1993).
[13] N. Cao, S. Chen, and Z.-S. She (unpublished); R. H. Kraichnan (private communication).
[14] G. Stolovitzky and K. R. Sreenivasan, Phys. Rev. E **48**, R33 (1993); R. Benzi (private communication).
[15] Z.-S. She and E. Leveque, Phys. Rev. Lett. **72**, 336 (1994).
[16] D. Lohse and A. Müller-Groeling, Phys. Rev. Lett. **74**, 1747 (1995); G. Falkovich, Phys. Fluids **6**, 1411 (1994); S. Grossman and D. Lohse, Phys. Rev. E **49**, 4044 (1994).
[17] C. W. Van Atta and W. Y. Chen, J. Fluid Mech. **44**, 145 (1970); S. G. Saddoughi and S. V. Veeravalli, J. Fluid Mech. **268**, 333 (1993).